necsa
We're in your world
RESEARCH AND DEVELOPMENT

PROJECT REPORT

Carbowaste
D-2.5.1

REMOVAL OF COATING LAYERS FROM TRISO PARTICLES BY LASER CUTTING

DOC No: NWR-CAWGEN-REP-12002
CW1303-D-2-5-1

Revision: 00

Author: WCMH MEYER

March 2013

TABLE OF CONTENTS

1 Executive Summary

Removal of Coating Layers from TRISO Particles by laser was researched as part of the international Carbowaste project. A Q-switched Nd:YAG laser system was employed for this processes as this type of technology was previously demonstrated at Necsa for the decontamination of metal surfaces.

The present report outlines the initial work done on surface decontamination with pulsed lasers. It consists basically of three parts:

(a) The relationship between ablation rate and laser fluence was investigated after optimal processing conditions were determined
(b) Testing of equipment by investigated the removal of a thin layer of metal from the surface of stainless steel (at this stage, without contamination).
(c) Finally, the cutting of a TRISO particle.

2 Introduction

2.1 Background

The objective of this project is the development of best practices in the retrieval, treatment and disposal of irradiated graphite (i-graphite) including other i-carbonaceous waste like structural material made of graphite or non-graphitised carbon bricks and fuel coatings (pyrocarbon, silicon carbide). It addresses both existing legacy waste as well as waste from graphite-based nuclear fuel (PBMR) resulting from a new generation of nuclear reactors.

The specific problem regarding the group of i-carbonaceous wastes stemming from the structures proposed by PBMR, is the possibility of long-lived radioisotopes like radiocarbon (^{14}C), chlorine (^{36}Cl), iodine (^{129}I), technetium (^{99}Tc), selenium (^{79}Se), cesium (^{135}Cs) etc. Resulting from activation processes during neutron irradiation. Therefore, this type of waste is handled as Intermediate-Level Waste (ILW), in most countries (LLW in France). Burning i-graphite might be an alternative to the disposal

option but will most probably not be politically accepted due to the radiocarbon releases to the environment if not separated or reduced in the exhaust gas. Recycling or reuse of treated i-graphite in the nuclear industry might be a preferred new option to minimize waste streams for disposal.

The CARBOWASTE consortium regards the present unsatisfactory status in this waste disposal area as an opportunity to build upon previous work, to review technological advances and innovative ideas which have arisen in more recent years, and thus to identify the most technologically appropriate, environmentally-sustainable, and cost-effective procedures, during all stages in the treatment and disposal of all types of carbonaceous wastes. The previously employed procedures are not necessarily appropriate for the future. Within this project, five principal investigations will ensure that the best-available and most environmentally acceptable technologies are identified in the following areas:

- An integrated waste management approach being compatible with ecological, economic and socio-political requirements, to be elaborated on in Work Package (WP1);
- retrieval procedures which might affect the nature of the waste (e.g. wet or dry) as well as the radiological and core integrity effects of retrieval over a range of time horizons. Methodologies for separation of coated particles from the PBMR fuel matrix, in the special case of V/HTR spent fuel (WP2) will also be considered;
- characterizing and then identifying suitable treatments for the carbonaceous wastes for removal of volatile and long-lived radioactive contamination associated with in-depth scientific investigations on microstructures and localisation of contamination including related analytical modelling (WP 3 & 4);
- elaboration of appropriate options for re-use and recycling of the graphitic materials, together with assessment of alternative options to bulk disposal in repositories (WP 5);
- investigations and further research and analysis on the disposal behaviour of i-carbonaceous wastes (WP 6).

2.2 Laser activity at Necsa

The research centre at NECSA is currently the technology Hub for Africa regarding the use of laser processes for the industry as well as nuclear industry. Historically Necsa had a collaboration agreement with Cogema on laser enrichment and Necsa expertise has build many specialized laser for these application. Technology gained at Necsa is also used to build commercial laser systems for the industry.

2.3 Laser literature

Laser cleaning is a relatively recent technique for removing pollutants from surfaces but is gaining popularity fast due to its advantages over other techniques. It is known that when laser intensity is high enough, especially in the case of high-power short-pulsed lasers, laser energy absorption occurs rapidly and only in a very thin layer on the target surface. This thin layer is thus instantaneously evaporated and removed without the use of any cleaning agents.

The merits of a laser cutting technique are firstly a remote application, since the laser beam can be delivered remotely via articulated mirrors or fiber optic cables while the ablation head can be manipulated by robots, thus avoiding exposion of workers and the laser system to possible radiation and/or contamination hazards.

Secondly, laser cutting only produces a small waste stream that can be easily handled by a scrubber or filter system, due to the fact that no cleaning agents such as detergents are needed.

We consider previous work done on different types of oxide layers, though by far the most interesting for the nuclear industry are those on stainless steel. Spencer et al (2000) note that 90 % of the radioactive contamination of stainless steel is confined to the top 100 μm of the surface. Further, this contamination is often predominantly in the surface oxide layer of the steel that, because of high temperatures and pressures in

many reactor conditions, are normally far thicker than the passive chromium oxide layer and, indeed, inhibit the formation of the latter.

Laser removal of oxygen films from stainless steel, prepared under similar conditions to those in a pressurized water reactor (PWR), was studied by Sato et al. (1997). They used a Q-switched Nd:YAG laser with a 50 mJ pulse energy and a pulse width of 12 ns. The oxide films were typically several μm thick. Measurements were also done on corrosion films that are typical of boiling water reactors (BWR).

X-ray photo-electron spectroscopy depth profiles of the oxide layer were measured before and after irradiation. The etch depths increased with laser fluence from a very low threshold of ≈ 0.25 Jcm^{-2} (i.e. far lower than the threshold for removal of the base metal). At a fluence of 2.3 Jcm^{-2}, the oxide film was almost totally removed from the substrate. It was found that element selective etching was not occurring by measuring depth profiles of chromium, iron and nickel as well as oxygen. The etching was compared at three harmonics i.e. 1064 nm, 532 nm and 355 nm. Results showed that the shorter the wavelength, the more effective was the etching for un-oxidised surfaces. However, for the oxide films there was no clear wavelength dependence for etching.

Removal of stainless steel oxide layers ("scales") of similar thickness to those found under reactor conditions (1 μm to 15 μm), but formed by hot-rolling or welding, was studied by Schluter et al (1996). The objectives were twofold. Firstly, in order to remove the scale (≈ 15 μm thick in hot-rolling, ≈ 1 μm thick in welding) by vapourisation to allow re-passivation of the surface. Secondly, re-melting of the surface to allow homogenization of the chromium concentration in order to improve pitting erosion resistance. The study was with CO_2 lasers: TEA, "pulsed CW" and CW.

The TEA CO_2 laser was found to be unsuitable for scale removal due to strong plasma absorption at the incident fluences needed for an efficient process. Operation of a CO_2 laser with long duration pulses (ie ≈ 100 μs c.f. ≈ 100 ns for the TEA) was found, however, to give efficient removal. To take advantage of the highest operating power, it was found best to use a CW CO_2 (up to 2.5 kW) laser scanning across the sample

sufficiently fast that the dwell time (≈ 55 μs) did not allow creation of a too deep heat affected zone. The most efficient removal was found on 1 μm thick WIG welding seams where a 750 W CW CO_2 laser achieved a de-scaling rate of 3.6 cm^2/s
(efficiency ~ 0.005 $\mu m.cm^2J^{-1}$)

Various studies on the removal of metal oxides by a laser were reported by Yavas, Oltra and Kerrec (1996) and by Oltra, Yavas and Kerrec (1997). Their oxide films of thickness ≤ 0.1 μm were produced on samples of iron or stainless steel under controlled oxidising conditions. These were radiated by a laser pulse transmitted through the electrolytic liquid in which they were immersed. The laser used was a Nd:YAG at 1064 nm with a pulse duration of 14 ns and a typical fluence of 0.6 Jcm^{-2}. The visible reflectivity of the sample surface was used to infer the degree of oxide removal (≈ 10% *with* the oxide layer and up to 90% *without* the layer). The removal was verified with energy dispersive x-ray spectroscopy (EDXS). They found efficient oxide film removal without any re-oxidisation when the laser pulse was applied with a negative applied potential on the sample and the electrolytic solution was basic. The fluence was sufficiently low that there was no melting or any other measurable change of the metal surface. Even without the laser pulse the oxide layer was removed, but on a far longer time scale. The reason for the enhanced removal was not understood. A potential use that was suggested for this method was the removal of radioactively contaminated layers in nuclear reactor vessels where lack of accessibility is a major problem.

Psyllaki and Oltra (2000) investigated the removal of Cr_2O_3 and Al_2O_3 from steel surfaces with a Nd:YAG laser with pulse duration 10 ns and pulse energy between 20 mJ and 60 mJ. These oxides were the result of high temperature oxidation of the surface of the steel. They found that the layer was removed completely from the surface in a single pulse by detachment rather than being vaporized or ablated. As a consequence, the mass loss was independent of the irradiation conditions, indicating a fixed layer thickness being removed by each pulse. They suggested that this could be due to acoustic waves at the oxide-metal interface or thermal shock of the surface. An important result was that rather low fluences could be used for removal i.e. in the range of only 1 Jcm^{-2} to 2 Jcm^{-2} for layers approximately 3 μm thick.

Further details of work done by Oltra and colleagues on oxide removal, including some details of diagnostic techniques and modelling, are given in Oltra et al (1996).

Removal of copper oxide layers has been studied by Wesner et al (1996) with an excimer laser and Kearns et al (1998) with a Q-switched Nd:YAG. While not of direct interest in nuclear decontamination, there are similarities with stainless steel oxide removal in so far as the different properties of the layer and substrate are concerned and the layers thicknesses.

Schluter et al. (1994) used both an ArF excimer laser at 193 nm with a pulse duration of 10 ns and a Nd:YAG at 532 nm (second harmonic) of pulse duration approximately 7 ns. The removal of the oxide layer was determined by x-ray photoelectron spectroscopy (XPS) using, in particular, the CuO and Cu_2O peaks at approximately 933 eV. These authors found increasing removal with fluence in air from a threshold of about 1.7 Jcm^{-2}, with improved wetability for solder for fluences up to 2.5 Jcm^{-2}. However, higher fluences lead to reduced wetability together with a marked change in the surface morphology as well as complete re-oxidation of the surface. In contrast, irradiation in an argon atmosphere and in a vacuum at similarly high fluences led to improved wetability in spite of changed morphology. This clearly indicating the undesirability of oxidation for wetability. They found that multiple pulse irradiation at weak fluences was more effective than single pulse irradiation to remove the copper oxide layer.

Kearns et al (1998) studied copper oxide removal with three harmonics of a Q-switched Nd:YAG (the first at 1064 nm, the second at 532 nm and the fourth at 266 nm). The pulse energies were 500 mJ, 250 mJ and 60 mJ respectively. The oxides comprised CuO and Cu_2O of which the latter was the main constituent in a layer approximately 0.3 μm thick. The low intensity absorption at 532 nm was considerably higher than at 1064 nm (i.e. 1-R = 92% c.f. 8%) more than compensating for the lower pulse energy at the shorter wavelength. However, this was not the case going to 266 nm (1-R = 80%).

The results were complicated by the strong spatial mode structure in the (single) laser pulses used. Nevertheless, removal of the oxide layer was found for fluences from 7.7 to 9.8 Jcm^{-2} at 1064 nm, 6.6 to 9.8 Jcm^{-2} at 532 nm and 2.7 to 4.2 Jcm^{-2} at 266 nm, i.e. progressively lower fluences as the wavelength decreased. "Explosive" removal features were seen at the two lower wavelengths suggesting mechanical as well as thermal effects were involved in removal. Overall it would appear that no improvement in removal was obtained in going to the UV wavelength (266 nm).

Summarising

For metal removal, the long pulse, free running, YAG was found to be by far the most suitable. Their longer pulses inhibit plasma formation and absorption for high pulse energies they are suitable for fibre optic beam transmission Nevertheless, very high fluences are needed for hole drilling while still higher fluences would be needed for the melt ejection required in the surface decontamination of metals. This means that for a reasonably large macroscopic area for the laser "footprint" on the metal, much larger pulse energies than the currently available 0.8 J would be desirable.

2.4 Aim of the project

The project is aimed at developing a technique, and the establishment of process parameters for the micro machining of coated Uranium fuel kernels to remove the coated layers of the fuel kernels in order to recover the Uranium Oxide (UO_2) core. The Uranium Oxide (UO_2) core with a diameter of ~500 µm, which is encapsulated with various coatings (Figure 1):

- Starting with porous graphite (~100µm)
- Pyrolitic graphite (~40µm)
- Silicon Carbide (SiC) (~35µm)
- Porous graphite (~35µm)

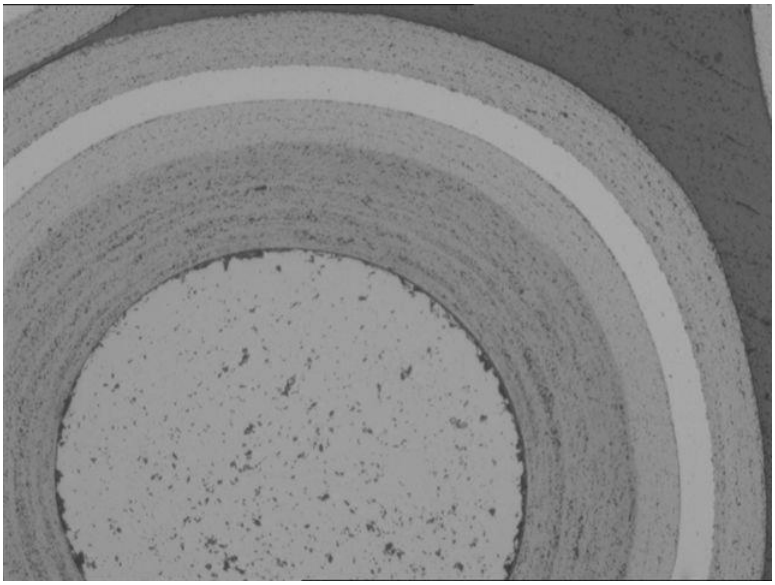

Figure 1. Macro photograph of a cross sectioned PBMR fuel kernel, showing the Uranium core with the various coatings.

3 Experimental work

3.1 Nd:YAG laser system

Turnkey systems for these applications are available on the market, doing a short survey and evaluating reliability of local laser equipment suppliers, it is suggested that making use of PK Welding & Robotics can be considered, the agent for Rofin lasers. The system shown in **Appendix A** would typically be capable of fulfilling cutting requirements.

Another turnkey system that should seriously be considered is a Dual beam Scanning Electron Microscope (SEM), with this system, the fuel kernels can be placed inside the instrument while precisely utilising the Focused Ion Beam (FIB) to generate superficial defects of < 5µm in diameter, or section the entire fuel kernel in half to examine the integrity of the coatings. The advantage of FIB cutting versus Laser cutting is that no heat is generated in the kernel that could have changed the properties of the coatings. The system shown in Appendix B is a very versatile SEM/FIB instrument.

The laser system used for the experiments at Necsa is a U.S. Laser Corporation (Model 406Q) Q-switched Nd:YAG laser. The Q-switch, which is an optical device utilizing Bragg diffraction to spoil the gain of the laser cavity, allowing loss modulation or "Q-switching", allows the laser to operate in a pulse train mode. The laser has four Q-control modes namely Internal Q, Gated Q, Triggered Q, and Gated CW (constant wave). The electronic control unit is used to vary the frequency from single pulse to 50 kHz.

The experimental setup that was used for this study is illustrated in Figure 2.

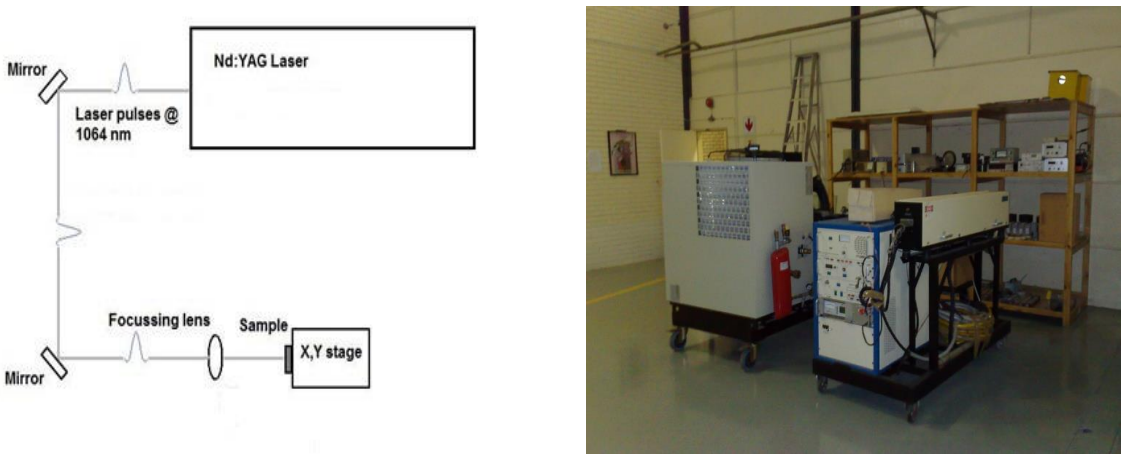

Figure 2. Experimental setup of Nd:YAG laser ablation system at Necsa.

A laser beam with a wavelength of 1064 nm, pulse duration of 67 – 220 nm (depending on the frequency), burst frequency of 0.01 – 50 kHz, and waist diameter of 4.1 mm, was produced at a lamp current of 35 Amperes. The laser beam was then focussed onto the target surface by a plano-convex lens with a focal length of 55 mm. The incident angle was set at 90°.

For the laser setup discussed above (Section 3.1) and the next with the fiber optic cable attached (Section 3.2), the focussed beam was used to cut graphite material at a specific point on a fixed graphite sample.

3.2 Nd:YAG laser system with fiber optics

For the fiber optic work, the experimental setup was similar to the one illustrated in Figure 2 except that the beam was delivered by a fiber optic cable instead of the conventional mirrors. The beam delivery system used in this study included the input coupler, gradient index fiber and the output coupler. The input coupler together with its mount assembly was responsible for positioning the fiber and focusing the laser beam into the fiber. An appropriate multi-element lens was used to focus the laser beam to a spot diameter small enough to fully couple the beam into the fiber core, which in this study was 800 µm. The lens was mounted in a three axis adjustable mount, which provided X /Y adjustment of the fiber, and a Z axis lens focus. Figure 3 shows the input coupler for the used laser system.

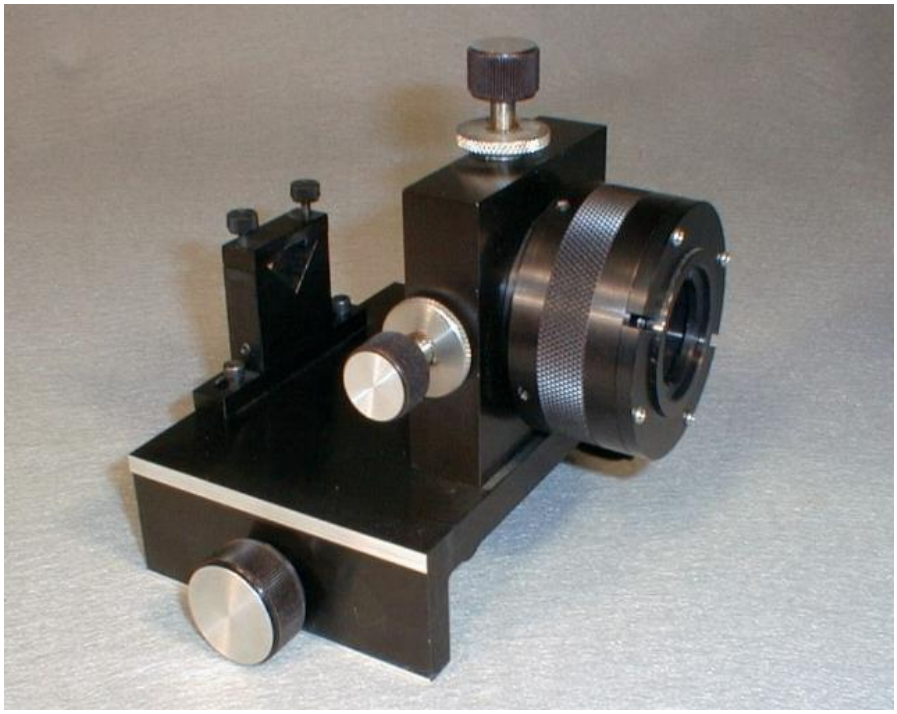

Figure 3. Input coupler for U.S Laser Corp Nd:YAG laser system.

The gradient index fiber optic cable, which had a doped fused silica core, had a core diameter starting at 1000 µm to 500 µm. Thus, the beam was focused inside the fiber optic cable in the same way a normal lens focuses a beam. The fiber is effectively lossless, except for approximately 8% Fresnel loss at the end faces.

The output coupler is a multi-element assembly which first collimates the diverging beam from the fiber output (the output collimator section), and then re-focuses it to form an image of the fiber core (the output objective assembly). A connector on the collimator assembly is provided for easy attachment of the fiber. The lenses are mounted in precision machined in-line housings, and are pre-aligned to the fiber. Figure 4 shows the output collimator assembly used for this laser system.

Figure 4. Output collimator for U.S Laser Corp Nd:YAG laser system.

4 Results

4.1 Determination of laser parameters

The first experiment performed was the measurement of laser power generated over the 0.01 – 50 kHz frequency range (Figure 5). This was done to determine what frequency corresponded to the maximum power output for this laser system. The Q-switch was set to internal-mode, which meant that the controller directly Q-switched the laser at the rate set on the digital panel meter.

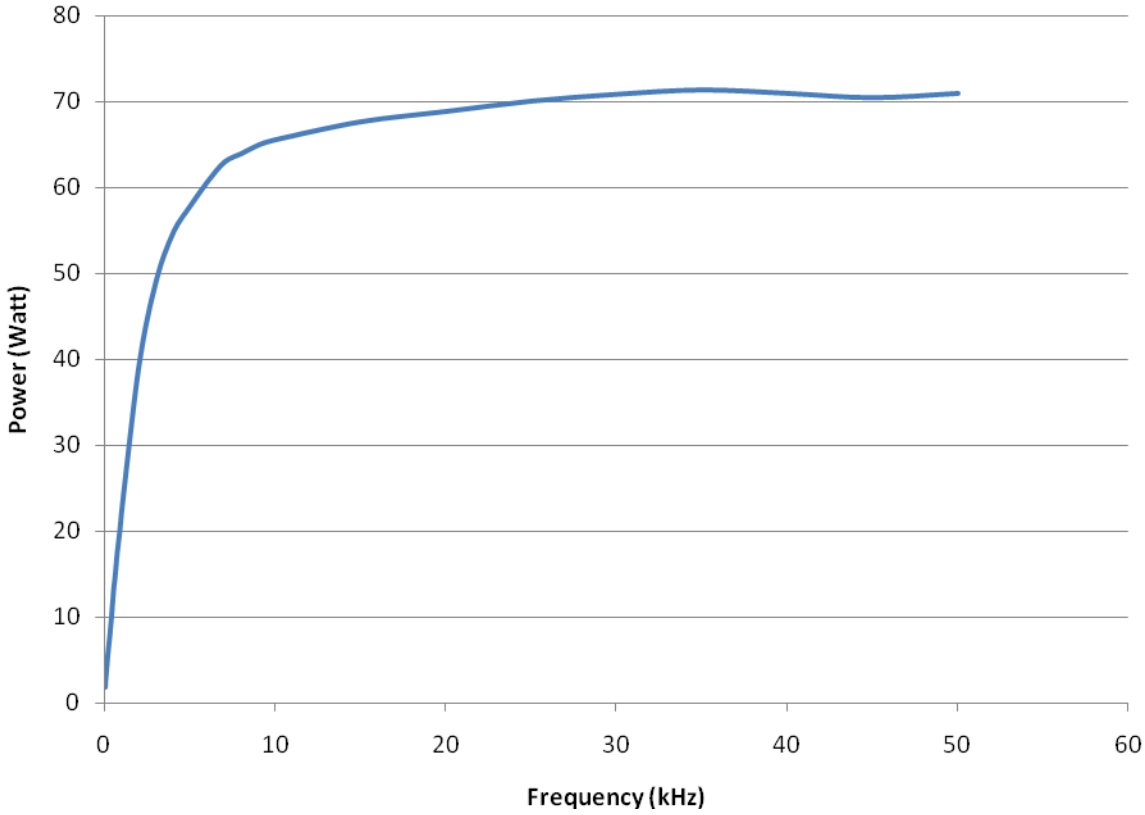

Figure 5: Average power in Watts versus the Q-switch frequency in kHz.

The results in Figure 5 suggested that the average power increased as the frequency increased, reaching a maximum average power of 71.4 W at 35 kHz. This suggested that the increase in pulses as the frequency was increased caused the overall power to increase up to 35 kHz. However, as the laser system comes closer to reaching its maximum frequency output the power starts to slowly decrease again. The pulse energy over the frequency range could then be determined as follows:

$$E = \frac{P_{Av}}{R_{Rate}} \quad (1)$$

Where: E = Energy in Joules

P_{Av} = Average power in Watts

R_{Rate} = Repitition rate in pulses per second

The calculated pulse energy against frequency is given in Figure 6.

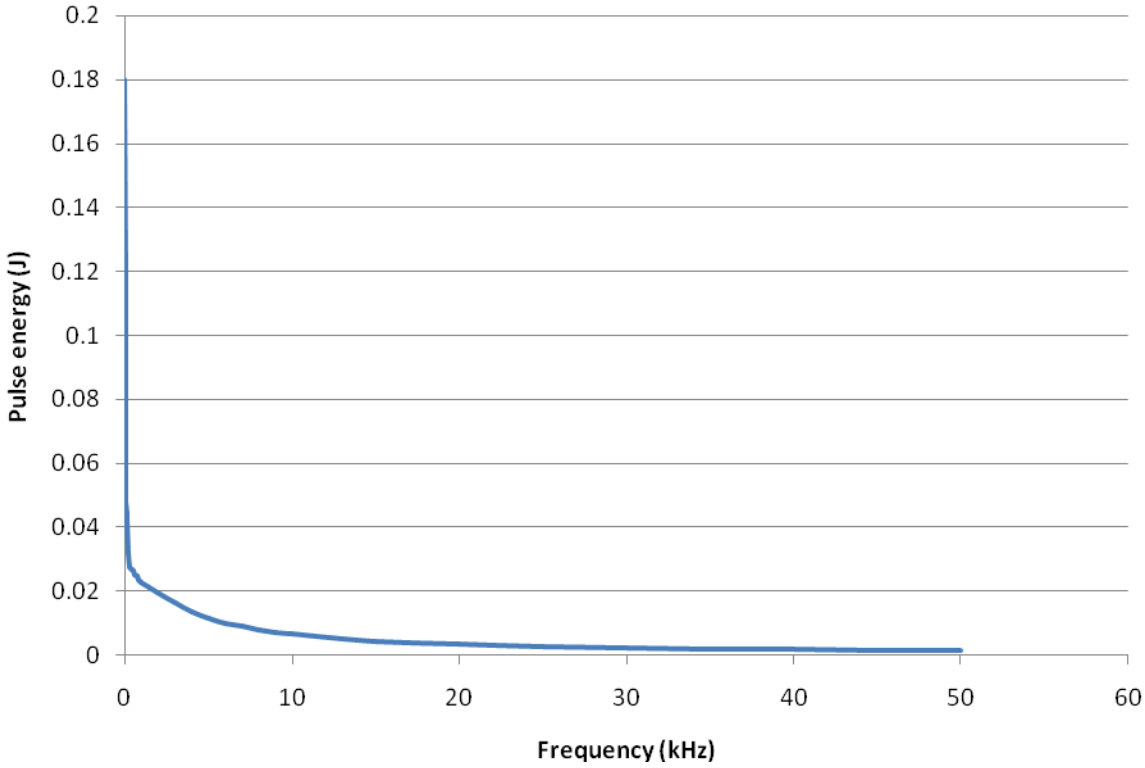

Figure 6: Pulse energy in Joule versus frequency in kHz.

The results in Figure 6 suggested that the energy per pulse decreased dramatically as the frequency increased reaching a maximum pulse energy of 0.18 J at 0.01 kHz and minimum of 0.00142 J at 50 kHz.

4.2 Metal surface layer removal by pulsed lasers

The excimer laser, as well as having a low removal efficiency, has too low an average power to be of interest in large-scale metal removal. Both the TEA CO_2 and the Q-switched YAG suffer from plasma absorption problems at the high fluences required, so that work on metal removal concentrated on the YAG in the free running mode.

The Q-switch was removed from the YAG by rotating the $\lambda/4$ plate through a quarter revolution. The pulse energy was reduced by approximately 2x so the on-sample fluence was recalibrated. However, the main difference was that the pulse duration was

now 50 μs (Figure 7) compared with 6 ns for the Q-switched mode, thereby considerably reducing the peak power (by ~ 10^4 x) for a given fluence.

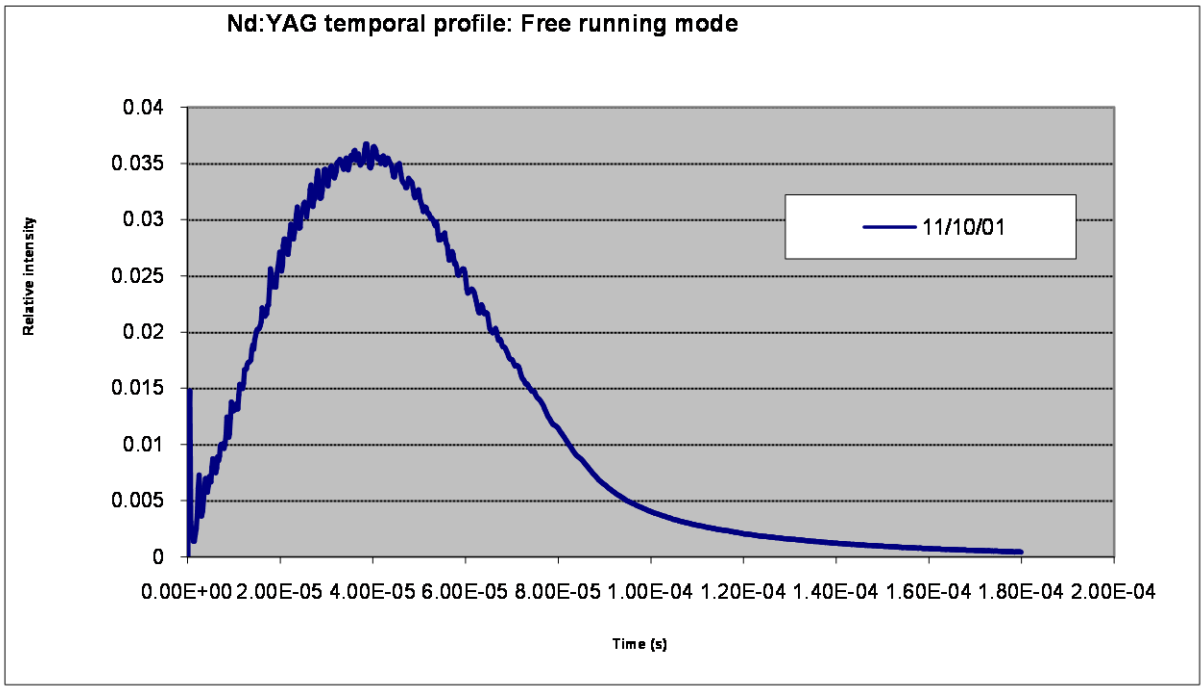

Figure 7: Temporal intensity profile of the Nd:YAG in free running mode.

By focusing a 5 mm aperture down to about 1 mm, a peak fluence of up to 30 Jcm^{-2} could be generated. Results for the removal efficiency obtained with drilling holes in 0.9 mm thick 304 L stainless steel with the free running YAG are in Figure 8. Clearly, high fluences ≥ 30 Jcm^{-2} are needed to achieve high removal efficiencies. This has the disadvantage, given the limited YAG pulse energy in the present work, that beam focus areas on the sample are rather small, ≤ 1 mm diameter.

It should be emphasized that these removal efficiencies refer to the volume of the hole. In fact much of this metal was melted and re-deposited at the edge of the entrance to the hole.

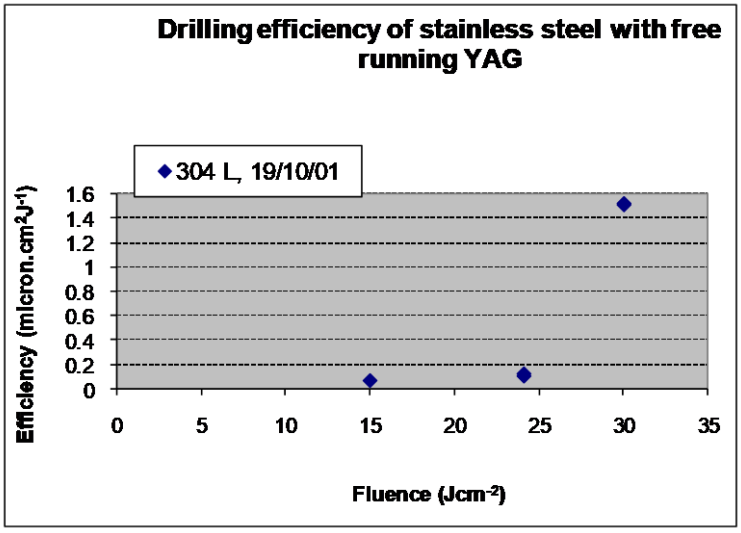

Figure 8: Drilling efficiency versus fluence for the Nd:YAG in free running mode

To achieve melt ejection to relatively large distances above the metal surfaces, in order to capture potentially contaminated metal, would require much higher vapour recoil pressures to be generated. Spencer et al (1996) found that this could be achieved with (Nd:YAG) laser power densities of $\geq$ 6 MW/cm^2 and pulse energies of 5 J with 1 to 10 ms duration. These figures correspond to very high fluences (c.f. figure 16) of $\geq$ 6 x 10^3 Jcm^{-2}. The effective "spot" size on the sample is still very small (< 1 mm diameter) and removal rates given by Spencer et al are in the range of 50 to 100 cm^2/kWhour for removal depths of order 0.5 mm. These correspond to removal efficiencies of only 0.007 to 0.014 μmcm^{2}J^{-1}.

It seems clear, therefore, that we will need higher pulse energies to achieve effective stainless steel removal over a reasonably large area

4.3 Laser cutting of triso particles without fiber optics

By using the plano-convex focussing lens, the beam was focussed to a spot size with a radius of 0.0221 cm and area of 0.00153 cm^2. The focussing of the beam helped to concentrate the energy from the laser, to achieve an energy density high enough for ablation. It should be noted that the pulse energy will stay constant at a certain frequency but the fluence (energy density) can be varied by just changing the spot size. The fluence/energy density (Figure 9) was then calculated at the different frequencies by means of equation 1.

$$F = \frac{E_p}{A} \quad (1)$$

Where: F = Fluence in J/cm^2

E_p = Pulse energy in Joules

A = Area of spot in cm^2

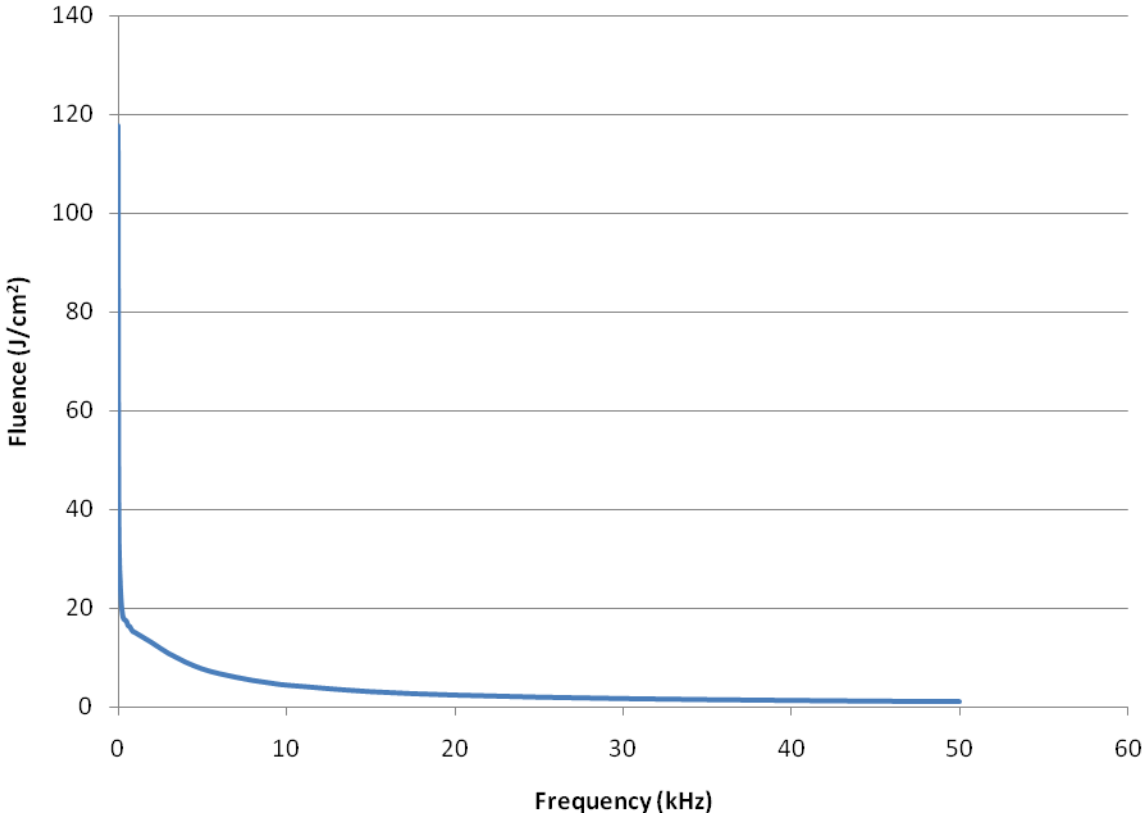

Figure 9: Calculated fluence of Nd:YAG laser at different frequencies.

The results suggested that the highest fluence of 117.647 J/cm^2 was measured at 10 Hz, which corresponded to the highest pulse energy.

Figure 10 shows the graphite sample after it was ablated at 10 Hz for the duration of 10 seconds. At this frequency and ablation time the total number of pulses was 100. It was the lowest frequency (except for single shot) and highest pulse energy that could be achieved with this laser.

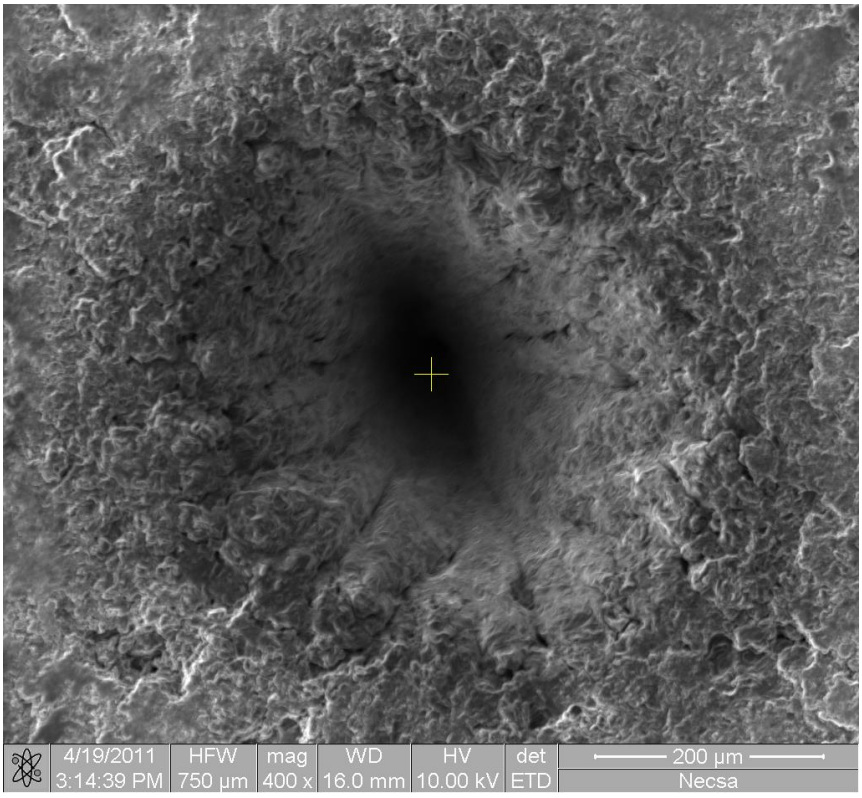

Figure 10: Ablation of graphite sample with focussed Nd:YAG laser at 10 Hz for 10 seconds.

The triso particles were cut using this system and the results in Figure 11 indicated that the current laser setup was suitable for cutting triso particles. However the cut was a bit wide and in order to reduce the width of the cut size, it was decided to study the use of fiber optics to solve this problem.

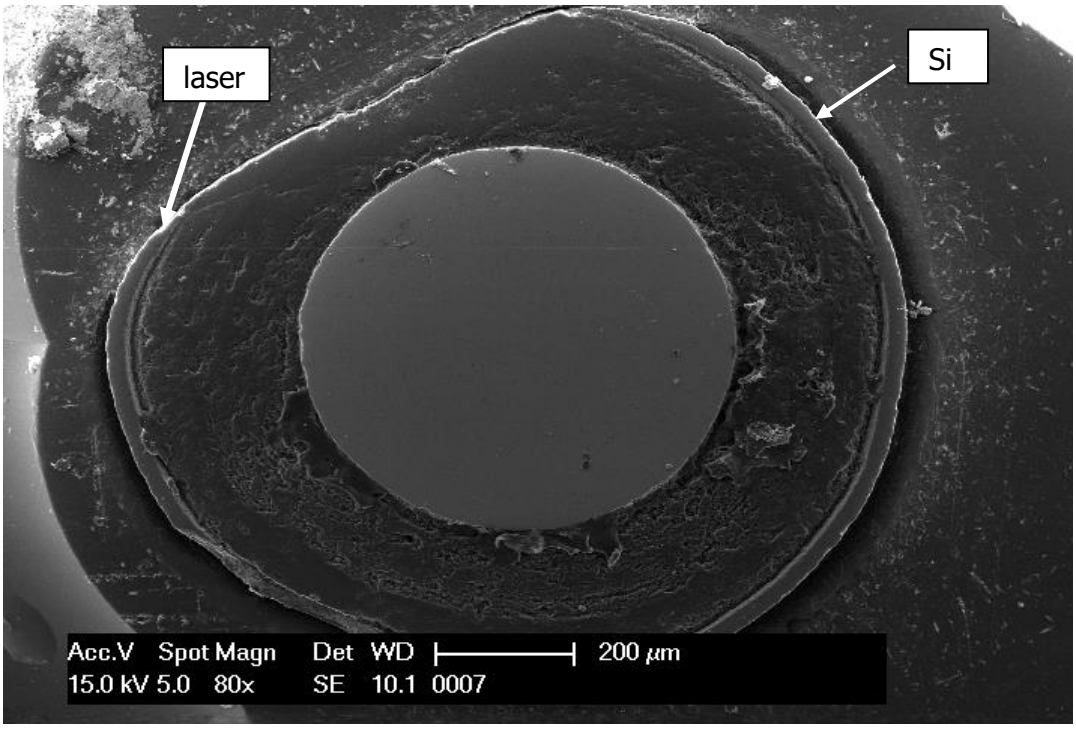

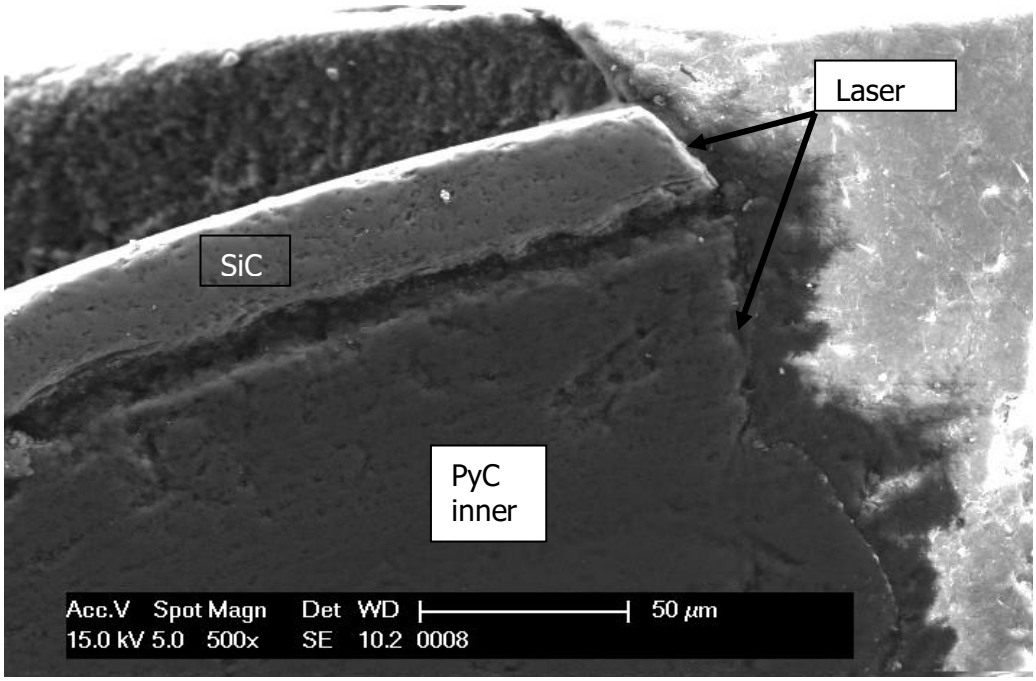

Figure 11: Laser cutting of triso particles using the plano-convex focussing lens

4.4 Laser cutting of triso particles using fiber optics

The beam delivery system used in this study included the input coupler, gradient index fiber and the output coupler.

The input coupler together with its mount assembly was responsible for positioning the fiber and focusing the laser beam into the fiber. An appropriate multi-element lens was used to focus the laser beam to a spot diameter small enough to fully couple the beam into the fiber core, which in this study was 800 µm. The lens was mounted in a three axis adjustable mount, which provided X /Y adjustment of the fiber, and a Z axis lens focus.

The output coupler is a multi-element assembly which first collimates the diverging beam from the fiber output (the output collimator section), and then re-focuses it to form an image of the fiber core (the output objective assembly). A connector on the collimator assembly is provided for easy attachment of the fiber.

The above setup did not only provide a medium in which the beam could be transported to the sample but also allowed the beam to be focused onto the sample. This ensured that the beam had a perfectly profile and allowed a much higher energy density (fluence) due to the fiber's profile (Figure 12). The fluence at 10 Hz was calculated at 141.73 J/cm^2 for an area of 1.27 × 10^{-3} cm^2. The area was calculated for a spot diameter of 402.54 µm. The depth of the ablated ditch (hole) was 805 µm, which gave a ditch volume of 1.02 × 10^{-4} cm^3.

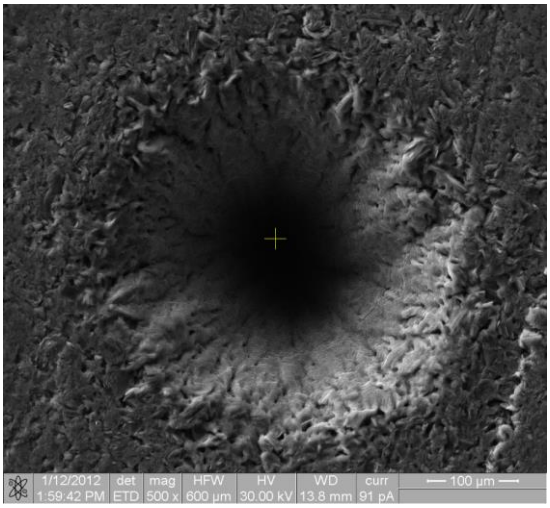

Figure 12. SEM photo of the graphite sample after laser ablation at 10 Hz for 10 seconds using a fiber optic cable.

The triso particles were cut using this fiber optic system consisting of a input coupler, gradient index fiber, the output coupler and a xyz translator. The results in Figure 13 indicated that with the current fiber optic setup the width of the cut on the triso particles were much smaller when compared when using the plano-convex focussing lens system.

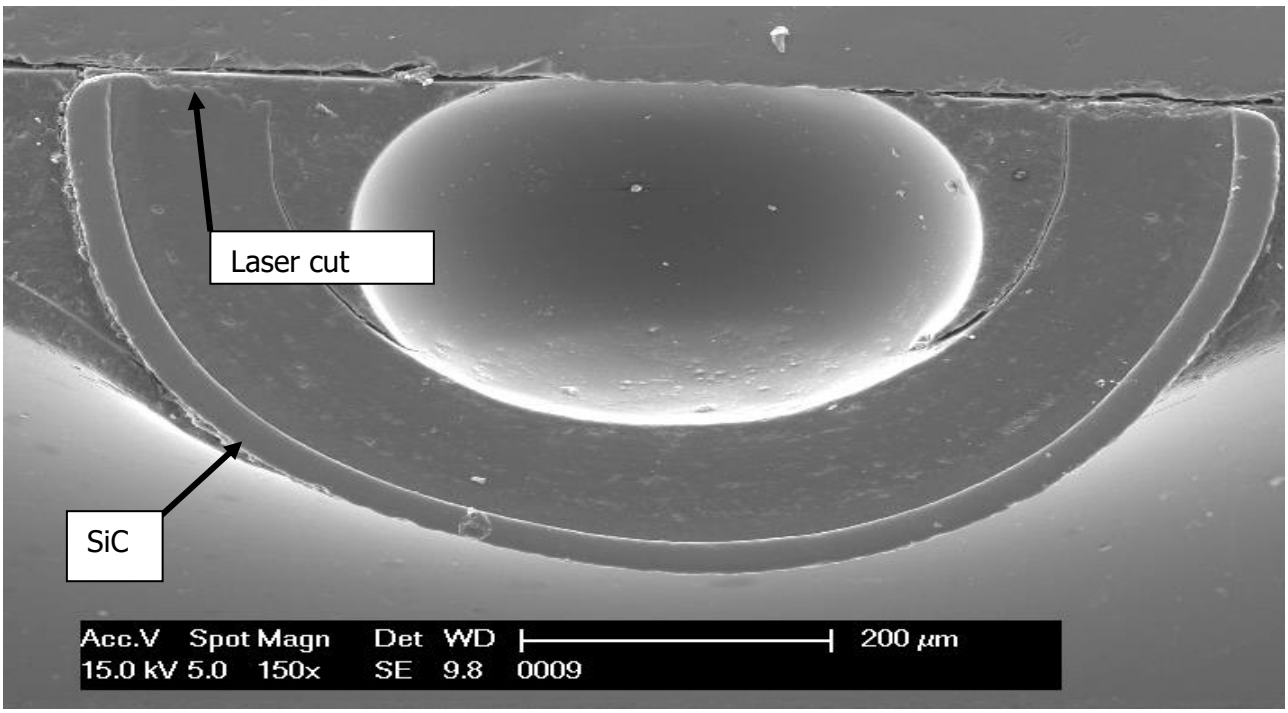

Figure 13: Laser cutting of triso particles using fiber optic system

With the fiber optic system confirmed for cutting, a triso particle was attached to a rotator and rotated to achieve a smooth cut through the different layers. The technology was further optimised (in terms of laser pulse energy, spot size, drilling time, rotation speed, etc.) on non-irradiated PBMR coated particles. After cutting through the SiC layer, the cutting process was stopped. The outer shell was removed where after the kernel was mechanically removed. The results in Figure 14 indicates that it is possible to make a very "smooth cut " through the SiC layer in order to remove the inside kernel.

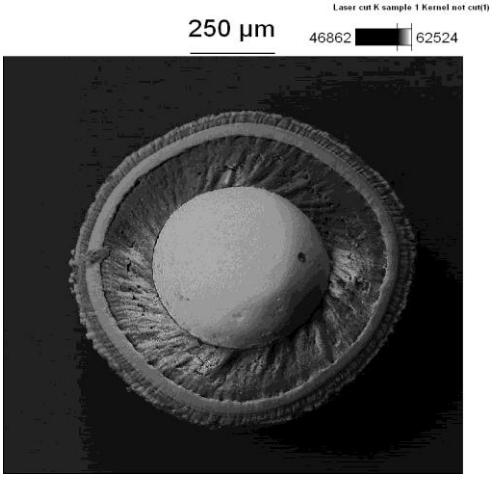

Figure 14: Cut through SiC layer and removal of the contaminated kernel

After removing the UO_2 kernel close examination of the layers could be investigated. The results in Figure 15 and Figure 16 indicated that limited acceptable "damage" to the different layers as no sintering or cracking can be observed.

Starting with porous graphite (~100µm): This layer was absent and can be attributed to the ablation process that took place during the initial cutting phase. The pyrolitic graphite (~40µm) was intact after cutting however a small piece of layer was missing. This is currently attributed to the handling of the sample for SEM analysis. The silicon Carbide (SiC) (~35µm) layer was also intact however a small piece of layer was "chipped" away. In this region it seems that the pyrolitic graphite layer is detaching form the SiC layer after the cutting process. The reason for this is currently unknown. The porous graphite (~35µm) inside the SiC layer seems intact after cutting

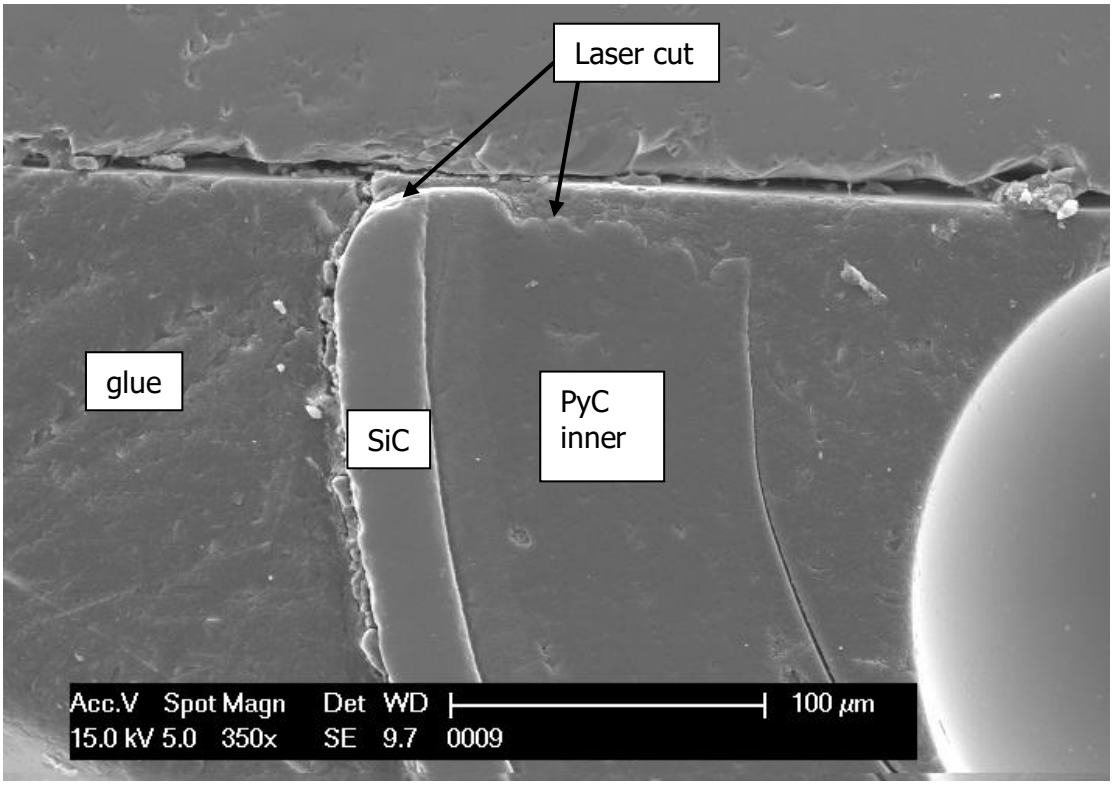

Figure 15: Integrity of triso particle layers after laser cutting

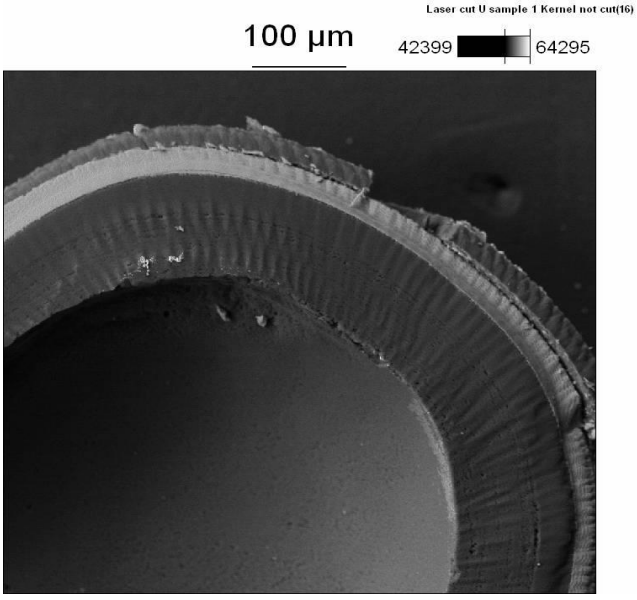

Figure 16: Integrity of triso particle layers after laser cutting

By adjusting the laser properties it is even possible to cut the kernel (e.g. UO_2) as indicated in Figure 17. As the cutting of the kernel is outside the scope of this project it will not be investigated further.

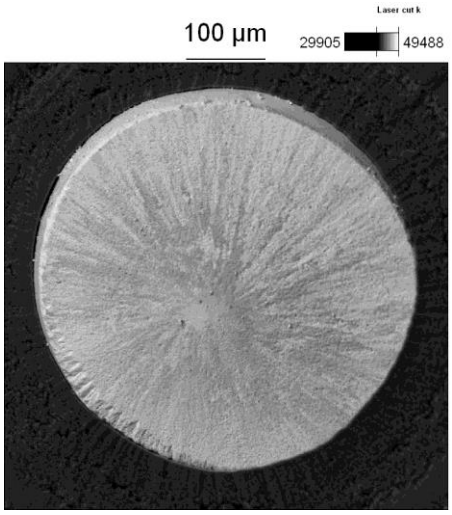

Figure 17: A UO_2 kernel cut in half using laser technology

5 Conclusion

As demonstrated in Section 4.3, it is possible and very efficient to use a Nd:YAG laser system to cut a triso particle. It was shown that the use of a fiber optic cable in conjunction with a focussing lens will enable the laser to cut or drill through the graphite material by only adjusting the focus of the beam (by means of the focussing lens) in accordance to the depth at which the graphite material is o be cut (ablated). It was also shown that the addition of an automated X, Y, Z translation stage would allow the precise cutting of small objects. The free running YAG, with approximately the same fluence as the Q-switched YAG but a far lower ($\sim 10^4$ x) peak intensity, is essential to avoid strong heat absorption into the graphite material as a result from plasma formation at the high fluencies. The results conclude that the laser system used in this study is a feasible and efficient to cut through the triso particle layers in order to remove the UO_2 kernel.

6 References

Kearns, A.; Fischer, C.; Watkins, K.G.; Glasmacher, M.; Kheyrandish, H.; Brown, A.; Steen, W.M. and Beahan, P., "Laser removal of oxides from a copper substrate using Q-switched Nd:YAG radiation at 1064 nm, 532 nm and 266 nm", Applied Surface Science, vol.127-129, 773 (1998).

Kerrec, O., "Enhancement of pulsed laser removal of metal oxides by electrochemical control", Appl. Phys., A63, 321 (1996).

Oltra, R.; Yavas, O.; Kerrec, O., "Pulsed laser cleaning of oxidized metallic surfaces in electrochemically controlled liquid confinement", Surface and Coatings Tech., 88, no.1-3, 157 (1997).

Oltra, R.; Yavas, O.; Cruz, F.; Boquillon, J.P. and Sartori, C., "Modelling and diagnostic of pulsed laser cleaning of oxidized metallic surfaces", Appl. Surf. Sci., 96-98, 484 (1996).

Psyllaki, P.; Oltra, R., "Preliminary study on the laser cleaning of stainless steels after high temperature oxidation", Mater. Sci. and Eng. A: Structural Materials: 282, No 1, 145 (2000).

Sato, S.; Shimizu, K.; Takashima, Y.; Soman, Y., "Laser etching characteristics of metal oxide films prepared under nuclear-reactor-water simulated conditions", Trans. IEE Japan, 117C, no.9, 1206 (1997).

Schluter, H.; Zwick, A.; Aden, M.; Uhlig, G.; Wissenbach, K. and Beyer, E., "Descaling of austenitic steels by laser radiation", (1994).

Spencer, J. T., Li, L., Modern, P. J., Steen, W. M. (BNFL Engineering Group); Potential applications of lasers for decontamination and decommissioning of nuclear plant; Euromat 96: Conference on Materials and Nuclear Power, p. 235-242; 1996.

Wesner, D.A.; Mertin, M.; Lupp, F. and Kreutz, E.W., "Cleaning of copper traces on circuit boards with excimer laser radiation", Appl. Surf. Sci. 96-98, 479 (1996).

Yavas, O.; Oltra, R.; Kerrec, O., "Enhancement of pulsed laser removal of metal oxides by electrochemical control", Appl. Phys., A63, 321 (1996)

7 Appendix

rofin - the innovative leader in the industrial laser market - 20.10.2005, 08:20 h
URL: http://www.rofin.com/english/products/micro-laser/starshape-laser/ss-e-d-l.php

StarShape E/D/L

Selective Ablation

The lasers of the StarShape E/D/L series accomplish precise and selective ablation of workpiece surfaces by vaporization processes – the ideal basis for micro structuring, drilling, cutting or scribing. Applications in the the photovoltaic, tool and mold making, semicon, automotive and medical device industries require processing of metals, semiconductors, ceramics or diamonds. Especially in this field the extremely good beam quality of the Q-switched solid-state laser proves ist advantage.

Nd:YAG or Nd:Vanadate

Depending on the structure size of the laser process you can choose between high-performance Gaussian mode (up to 20 W) or low order mode lasers (up to 100 W) with a wavelength of 1064 nm. As to applications with extremely critical heat affected zones the Nd:Vanadate laser – the StarShape E is the optimal system. Its extremely short laser pulses minimize the draining of the energy via heat conduction. The result is an almost optimal process efficiency and minimal thermal load, which is ideal for micro structuring. In case of greater ablation volumes however, the longer pulses of the lamp or diode-pumped Nd:YAG lasers – StarShape D and L – have proven their efficiency.

Also in Green

Certain materials like copper or various semiconductors show absorption characteristics, different from other materials. Green light (532 nm) used here in frequency-doubled lasers has a decisive advantage: the absorption is significantly higher and therefore the laser power can be injected very efficiently into the material surface to be processed.

Flexiblity

Dynamic beam technology is the optimal choice if speed is required, since the laser beam can be moved much faster than a heavy workpiece. Of course, all the lasers can also be equipped with fixed optics - some with flexible fibercoupling.

Various power levels, wavelengths, pulse widths and flexible equipment – StarShape solid-state lasers cover a huge range of applications. Specify yours!

Quanta™ 200 3D

Key Benefits

- Multi vacuum mode enables in-situ dynamic experiments and imaging and analysis on any sample.
- Tungsten electron source is ideal for analytical techniques such as EDS.
- SPI mode for monitoring FIB patterning process.
- Integrated digital patterning engine allows optimized patenting conditions for each application, production of complex shapes and 3D milling.
- Accurate, efficient and easy-to-use automation software.
- Versatile system allows a wide range of accessories for analysis and sample manipulation.

The Quanta 200 3D DualBeam (FIB / SEM) is ideally suited to the industrial process control lab that must image or analyze multiple cross sections in challenging samples. For the materials science lab it offers the capability of in-situ dynamic experiments, 3D imaging and analysis and TEM sample preparation for more in-depth analysis. The multi-vacuum mode (including ESEM), coupled with the ability to attach a cryogenic stage, offers life science labs a unique way of collecting information even from the most challenging of samples.

The Quanta 3D, with its tungsten electron column, focused ion beam column and gas injector system, is a full DualBeam offering all of the capabilities of site-specific cross

sectioning, complex ion beam patterning, material deposition and etching, imaging and analysis. The multi-vacuum mode offers researchers the ability to conduct in-situ dynamic experiments in wet, cold or high temperature conditions and image or analyze any sample without charging.